10th Brazilian Congress on Manufacturing Engineering
August 05th-07th, 2019, São Carlos, SP, Brazil

IN-SITU AGED LASER WELDED MARAGING STEELS

Milton Sergio Fernandes de Lima
Rafael Humberto de Mota Siqueira
Sheila Medeiros de Carvalho
Antonio Jorge Abdalla
Photonics Division, Institute for Advanced Studies, Trevo Amarante 1, 12228-001 São José dos Campos, SP, Brazil.
E-mails: miltonsflima@gmail.com; rhmotasiqueira@gmail.com; sheila_mcarvalho@yahoo.com.br; ajorgeabdalla@gmail.com

Abstract. *Maraging steels have been used in many applications in aerospace due to their high specific mechanical strength. Nevertheless, welding is a challenge because of the local softening in the fusion and heat-affected zones. In order to increase the hardness of these zones, a post-welding heat treatment using a laser is proposed, i.e. the same laser responsible for the weld reheats the joint producing localized aging. Three mm thick 18 Ni 300 maraging steel coupons were bead-on-plate welded using 1800 W and speeds of 1.8, 2.4 and 3.0 m/min. Laser heat treatment was carried out using a 2 mm defocused beam, power of 130 W and scanning speed of 10 mm/min. Using this method, the hardness at the middle of the fusion zone increased from 270 to 340 HV, which is similar to the base material. According to the simulations, the laser post-welding heat treatment attained temperatures around 1000°C in the middle of the fusion zone with a period of 130 seconds above 500°C. The laser reheating induced the precipitation of an inter-dendritic intermetallic layer and tempered the intra-dendritic martensite. This method was proven useful for in-situ aging without need of further furnace treatments.*

Keywords: *laser beam welding, ultra-high strength steels, maraging steels, post-welding heat treatments.*

1. INTRODUCTION

Maraging steel 18 Ni 300 is widely used in the aerospace industry in applications requiring high mechanical strength. Unlike ordinary carbon steels, these alloys usually present soft martensite micro-constituents which attain high levels of mechanical strength after aging. The precipitation hardening in martensitic maraging grains is known to occur between 315°C and 540°C (ASM, 1990) although the actual intermetallic precipitates are still in discussion (γ - Ni_3Mo, η - Ni_3Ti, Laves - Fe_2Mo, σ- FeMo, μ - Fe_7Mo_6, FeTi, Fe_2Ti, etc.) (Sha, 2009; Tariq, 2010).

A number of studies were dedicated to the weldability of maraging steel 18 Ni 300. Fanton et al. (2014) reported laser welded 18 Ni 300 steel has two main issues: the softening of the fusion zone (FZ) and the appearance of reverted austenite. The FZ softening, extensive to the heat-affected zone, is intrinsic to any welding method because of the dissolution of the precipitates at high temperatures. The reverted austenite formed in the inter-dendritic areas of FZ cannot be hardened by aging, having inferior strength and hardness compared to the aged martensite. The same authors indicate that a post-welding heat treatment (PWHT) at 480°C per 1 h equalizes the hardness of the FZ near to the base material (BM).

Large metal welded components are difficult to treat because of the weight and the temperature differences inside the furnace. Additionally, PWHT of welded maraging steels can eventually overage the base material and then cause local softening far the weld bead (Fanton et al., 2014). One possible solution is to use the laser itself as a heat source for PWHT. Using this technique, a low power low scanning speed beam moves though the weld path to reheat the region. Under very controlled conditions, the method could avoid expensive PWHT in furnaces by aging the as-solidified steel. To the knowledge of the authors, it is the first time for the use of laser as a source of PWHT.

The aim of this contribution is evaluate the use of an in-situ heat treatment of laser welded maraging steel 18 Ni 300 using laser post-heating. The microstructures after welding and after PWHT were analyzed by optical microscopy and the mechanical behavior by Vickers hardness measurements.

2. EXPERIMENTAL

The base material is an 18 Ni 300 maraging steel with composition given in Table 1. The as-received blanks had 3 mm thickness and were furnished in solubilized and aged conditions.

Laser beam welding (LBW) were performed in the Laser Applications Lab of IEAv (Institute for Advanced Studies, São José dos Campos, SP) using a 2 kW Yb:fiber laser (IPG, YLR-2000). The laser workstation consisted of the optical fiber, a weld head and a CNC table. The laser power was fixed at 1800 W and the weld speed was 1.8, 2.4 and 3.0

m/min, in agreement of a number of preliminary room temperature tests. The laser welds were realized bead on plate in a single run.

Table 1. Chemical composition of the base steel (wt.%, Fe balance).

C	Si	Mn	Ni	Mo	Co	Al	Ti
0.005	0.050	0.050	18.5	5.0	8.80	0.11	0.70

The post-weld heat treatment (PWHT) was carried out with the same laser but with reduced speed and power and an enlarged beam diameter in order to produce local heating. A number of experiments was carried out to observe the laser damage at the surface and then the following process parameters were fixed: beam diameter 2 mm, laser power 130 W and scan speed of 10 mm/min. One set of experiments using LBW in room temperature, without heat treatment, was carried out for comparative purposes.

The obtained microstructures were analyzed by optical microscopy using standard polishing techniques and Nital 2% (2% nitric acid in ethanol) etching. Metallographic analyses were carried out using ImageJ® software. The microscope was a Zeiss model Imager2M and the scanning electron microscope (SEM) was a Hitachi TM-3000. The mechanical behavior was estimated using a Vickers indenter with 200 gf load and dwell time of 10 seconds. Thermodynamic calculations were carried out using ThermoCalc® software version L. The database was the FEDAT TCS/TT Steels Database v1.

Thermal simulations were carried out using SysWeld Software©, a finite element analysis software designed for welding and heat treatment of metals and alloys. For the current purposes, a refined mesh around the laser path was designed and the desired output was the time-temperature evolution during weld and PWHT. The exact maraging steel properties are unavailable in the Sysweld database, therefore DC04 steel properties were used instead.

3. RESULTS AND DISCUSSION

3.1 Room temperature LBW

Laser welds performed at room temperature have macroscopic characteristics such as those observed in Fig. 1. In general, the fusion zones (FZ) were thinner and deeper as the speed varies from 1.8 to 3.0 m/min. The weld obtained at 1.8 m/min has a top width of 2.15 mm and penetration of 2.5 mm. The weld obtained at 2.4 m/min has a top width of 1.76 mm and penetration of 2.4 mm. The weld obtained at 3.0 m/min has a top width of 1.25 mm and penetration of 2.7 mm. The top width of the bead decreased with increasing speed because the plasma generated on the surface is more intense with slower speeds, since the interaction time increased and more metallic ions were present. Additionally, as speed increases, the plasma plume tends to move backwards of the keyhole, allowing the incident beam to penetrate deeper into the base material (BM). This effect is known and reported as a function of the gaseous flow causing the plasma to move away from the center of the beam (Ahn et al., 2017).

The extent of the heat-affected zone (HAZ) is a function of the welding speed, although it varies depending on the region where it was measured. In the case of the macrographs shown in Fig. 1, the HAZ in the keyhole surroundings varies between 0.7 and 0.4 mm, from 1.8 to 3.0 m/min. This region is equivalent to the limit of dissolution of intermetallic precipitates responsible for the material hardening.

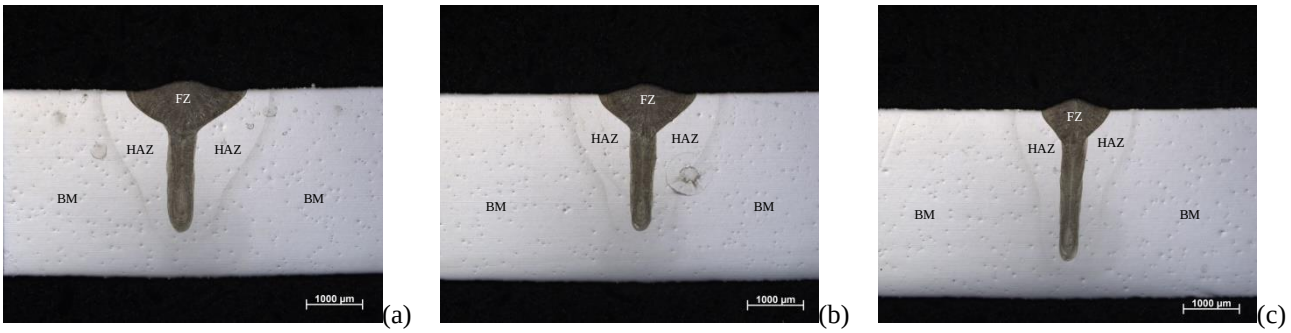

Figure 1. Macrographs of the welds obtained at room temperature: (a) 1.8 m/min; (b) 2.4 m/min e (c) 3.0 m/min. BM = base material, HAZ = heat-affected zone and FZ = fusion zone.

The microstructure of the FZ is similar for the three weld speeds, and characterized by columnar dendritic grains as depicted in Fig. 2. The average secondary dendrite spacing was 1.6 µm and the interdendritic micro-segregation accounted by 21.4% of the surface area in Fig. 2. According to ThermoCalc simulations, the partition coefficients of Ni and Co are almost one, and Mo and Al are 0.7 and 0.8, respectively. The most important element segregated to the

inter-dendritic spaces is Ti with partition coefficient of 0.4. These compositional differences indicate an interdendritic space relatively rich in Ti, which increases the potential for intermetallic nucleation during aging.

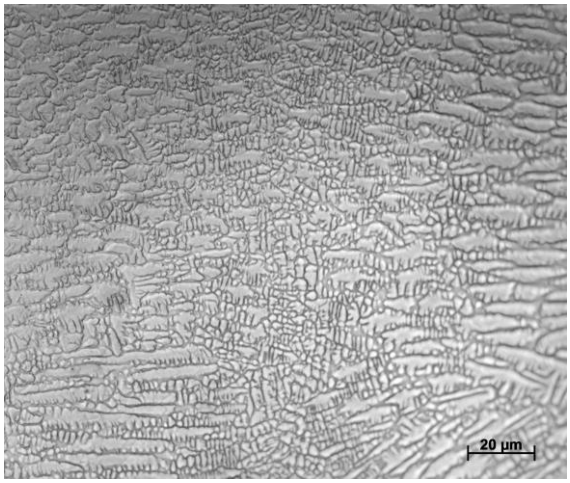

Figure 2. (a) Dendritic structure at the middle of the FZ, sample 1.8 m/min. (b)

Figure 3a presents a comparison between experimental (micrograph at right) and theoretical (simulation at left) for the coupon welded at 1.8 m/min. Although the match is not perfect, one could easily differentiate FZ and HAZ from the 1500°C isotherm. The numbers one to four in Figure 3a are representative of the fusion zone, fusion line, and heat affected zone as plotted in Figure 3b. As can be seen, the zone marked 1 and 2 exceeded the *liquidus* temperature (1444°C, as given by ThermoCalc) and then a dendritic as-solidified structure was expect, Fig. 2. The regions 3 and 4 presented a peak temperature of 1300°C and 956°C, respectively. These temperatures are above minimum annealing temperature of 860°C (Lima Filho, 2016) and thus regions 3 and 4 correspond for a light gray band in Figure 3a. Independently of the region, the cooling rates around 500°C, between 208 and 297 °C/s, avoid any precipitation due to the nucleation kinetics. As a result of the solubilization, the hardness in FZ and HAZ (light gray band in Figure 3a) decreased from 340 HV (BM) to 270 HV (FZ), as presented in Fig. 4.

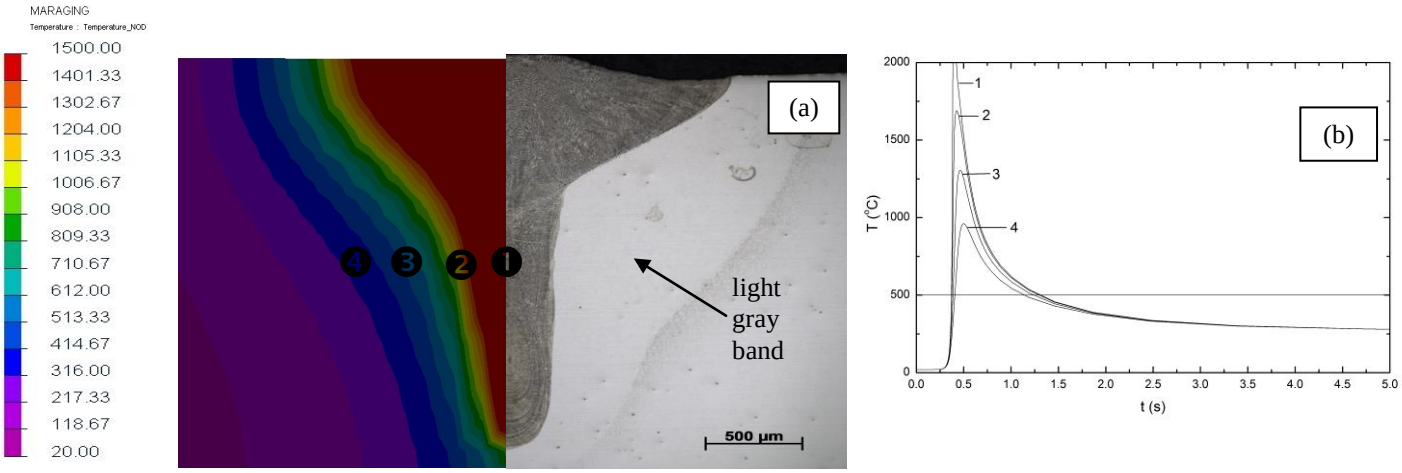

Figure 3. Sysweld results: (a) comparison between simulation and weld cross section for condition 1.8 m/min. (b) temperature profile three indicated regions.

3.2 Laser-heated LBW

Figure 5a shows a macrographic cross-section of the sample after laser PWHT superposed to the hardness profile. Comparing Figure 5a to Fig. 4 evidences the increasing in hardness due to the laser treatment after welding. The average hardness in the same regions in the middle of FZ increased from 270 to 340 HV. The base material near to the heating region also increased the hardness from 330 to 400 HV. The reasons for the in-situ aging can be explained in Figure 5b as obtained by FEM simulations. The temperature profiles for three regions marked 1, 2 and 3 in Figure 5a

were plotted considering the laser weld, time between 0 and 3 seconds, and laser PWHT, time between 15 and 200 seconds. As can be seen, the region 1 attained temperatures exceeding *liquidus* (1444°C) and then it melted during the treatment. Consequently the region 1 in Figure 5a presented some ablation when compared to Fig. 4. The peak temperatures in region 2 and 3 are 1079°C and 951°C, respectively. These temperatures exceed solubilization however the cooling rate was greatly reduced compared to the laser weld.

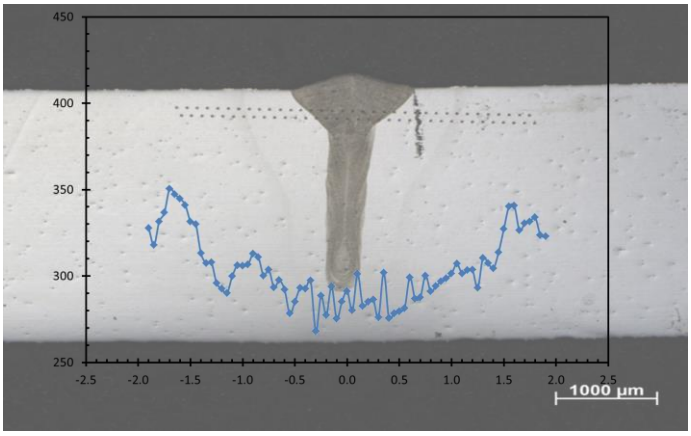

Figure 4. Hardness profile together with related sample cross section (cond. 1.8 m/min)

The 18 Ni 300 steel aging is known to occur at temperatures between 315°C and 540°C in isothermal periods ranging from 5 minutes to 5 hours (Lombardo, 2015). However it occurred much faster in present investigation as can be seen by the calculated temperatures (Figure 5b). Theoretically, there are two reasons for the accelerate aging: metastable structure and the heating-cooling cycles. First, the solidified material presented in a metastable form with chemical modulations proud to create precipitates at a right distance. This distance could be approximately 1.6 µm as shown before. Second, the heating and cooling periods exceeded the precipitation range but were too fast to diffuse long distance solutes, such as those necessary for revert austenite. Although the period above 500°C was only 130 seconds, it was sufficient to ignite precipitation in the martensitic branches, as can be seem in Figure 6.

Figure 6 shows a scanning electron micrograph next to the region marked 2 in Figure 5a. As titanium was segregated to the inter-dendritic spaces during solidification, laser PWHT gave sufficient energy to growth an intermetallic layer, around 0.5 µm thick, among the dendrite branches. The intra-dendritic material was tempered as presented in Figure 6 as well. The composition of the intermetallics, both intra and inter-dendritic, are unknown by now.

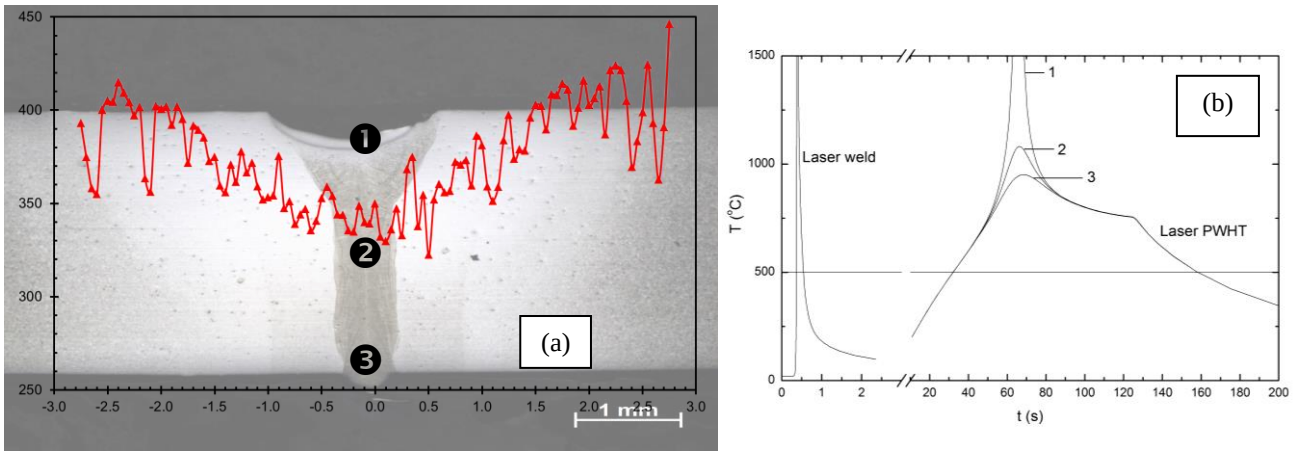

Figure 5. (a) Hardness profile together with related sample cross section (cond. 1.8 m/min plus PWHT), (b) Prediction of weld and PWHT for the condition 1.8 m/min. The numbers are related to the different regions at the top, middle and bottom of the weld bead.

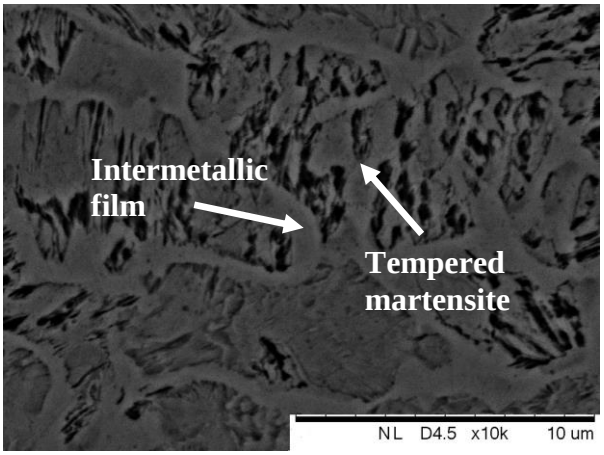

Figure 6. SEM image of a region around number 2 (Figure 5a).

4. CONCLUSIONS

The following conclusions can be drawn:

Laser beam welding produce defect-free bead-on-plate welds for a 3 mm thick 18 Ni 300 maraging steel with laser power of 1800 W and speeds of 1.8, 2.4 and 3.0 m/min.

The fusion zone microstructure was characterized by dendritic growth of austenite, transformed to martensite on cooling. According to ThermoCalc, the inter-dendritic spaces are rich in Ti.

The laser welds caused depletion in hardness in the fusion zone and heat-affected zone from 340 to 270 HV, as previewed by FEM simulations.

The laser post-welding heat treatment attained temperatures around 1000°C in the middle of the fusion zone with a period above 500°C of 130 seconds, according to the simulations.

The laser reheating induced the precipitation of an inter-dendritic intermetallic layer and tempered the intra-dendritic martensite. These effects induced an increase of hardness from 270 HV to 340 HV in the fusion zone.

This method was proven useful for in-situ aging without need of further furnace treatments.

5. ACKNOWLEDGEMENTS

This research has been supported by Fundação de Amparo à Pesquisa do Estado de São Paulo (FAPESP) under grant number 2016/16683-8.

6. REFERENCES

Ahn, J., He, E., Chen, L., Dear, J and Davies, C.M., 2017. "The effect of Ar and He shielding gas on fibre laser weld shape and microstructure in AA 2024-T3". J. Manufacturing Processes, Vol. 29, p. 62-73.

ASM, 1990, *Metals Handbook: Volume 1: Properties and Selection: Irons, Steels, and High-Performance Alloys*, ASM International, Novelty OH, 10th ed.

Fanton, L., Abdalla A. J., and Lima, M.S.F. 2014. "Heat Treatment and Yb:Fiber Laser Welding of a Maraging Steel". Welding Journal, Vol. 93, p. 362-s- 368-s.

Lima Filho, V. X., Barros, I. F. and Abreu, H. F. Gomes de., 2017. "Influence of Solution Annealing on Microstructure and Mechanical Properties of Maraging 300 Steel". Materials Research, Vol. 20(1), p. 10-14.

Lombardo, S., 2015, Caracterização Mecânica e Microestrutural de Juntas Soldadas a Laser em Aços Maraging com Posterior Tratamento Térmico e Termoquímico de Superfície a Plasma, Thesis PhD, Faculdade de Engenharia do Campus de Guaratinguetá, Universidade Estadual Paulista, 193p.

Sha, W. and Guo, Z., 2009. *Maraging steels: Modelling of microstructure, properties and applications***.** Woodhead Publishing Limited, Cambridge. ISBN 978-1-84569-686-3.

Tariq, F., Naz, N. and Baloch, R.A., 2010. "Effect of Cyclic Aging on Mechanical Properties and Microstructure of Maraging Steel 250". Journal of Materials Engineering and Performance. Vol. 19(7), p. 1005–1014.

7. RESPONSIBILITY NOTICE

The authors are the only responsible for the printed material included in this paper.